ASIA-PACIFIC JOURNAL OF CHEMICAL ENGINEERING
Asia-Pac. J. Chem. Eng. 2008; **3**: 550–559
Published online 27 August 2008 in Wiley InterScience
(www.interscience.wiley.com) DOI:10.1002/apj.179

Curtin University of Technology

Research Article

Effect of promoters and secondary fluidizing medium on mixing: statistical and ANN approaches

Y. K. Mohanty,[1] B. P. Mohanty,[1] G. K. Roy[2] and K. C. Biswal[2]*

[1] *Department of Chemical Engineering, G.I.E.T., Gunupur, Rayagada, Orissa, India*
[2] *Department of Chemical Engineering, N.I.T, Rourkela, Orissa, India*

Received 21 March 2008; Revised 17 June 2008; Accepted 23 June 2008

ABSTRACT: Factorial design (statistical approach) and artificial neural network (ANN) models have been developed for the prediction of mixing the index with four system parameters, such as static bed heights, average particle densities, average particle sizes and gas velocities, under four different experimental conditions, *viz.*, only primary air, simultaneous primary and secondary air, disc promoter and rod promoter. The values of the mixing index obtained through the developed models are found to agree well with their experimental counterparts. It has also been found from these investigations that under simultaneous primary and secondary air supply conditions the best mixing performance is achieved, i.e. $I_M \approx 1.0$, as compared to rod promoter, disc promoter, and only primary air supply. © 2008 Curtin University of Technology and John Wiley & Sons, Ltd.

KEYWORDS: mixing; factorial design; fluidization; promoter; secondary air; artificial neural network

INTRODUCTION

The need to develop a model for predicting the behavior of a system arises in a number of disciplines. In engineering, models of physical system are required for solving prediction, control, diagnosis and design problems. Generally, the gas–solid fluidized beds have excellent and rapid mixing characteristics for segregating particle systems. Particle separation phenomenon is not uncommon in industrial fluidized beds, where particles of widely different sizes or densities are handled. Fluidized bed reactors that can be operated in different modes either to promote particle mixing or to enhance particle segregation have been studied. It is also not unusual to have one part of the fluidized bed reactor operated in a mixing mode while the other in a segregating one.

A qualitative model for particle mixing in a gas fluidized bed was developed by Gibilaro and Rowe[1] based on four physical mechanisms: overall particle circulation, interchange between wake and bulk phases, axial dispersion and segregation.

Grace[2] reported that most of the gas fluidized beds that are operated in bubbling or turbulent fluidization regimes contain nonuniform mixtures of particles. Further, Rowe and Nienow[3] reported that in some cases, solid materials (reactants or catalysts) are composed of different sizes and/or densities, whereas according to Aznar *et al*.[4] the binary or multi-solid systems are sometimes formed by the addition of other types of solids that differ from the original bed material. Bi *et al*.[5] studied that to increase the holdup of the fines, and to improve the contact between gas and fine solids in transport risers, addition of coarse particles may also be necessary. Research on the hydrodynamic behavior of fluidized beds containing nonuniform mixtures of particles has so far largely been confined to binary mixtures only. Nienow *et al*.[6] and Hoffmann *et al*.[7] reported from their studies that most of these research works have paid attention to the solid mixing and segregation that are expected in the relatively lower gas velocity range.

Noda *et al*.[8] studied the minimum fluidization velocity of binary mixtures of particles with large size ratios and found that the minimum fluidization can be correlated as a function of composition and the ratios of densities and sizes.

Fan *et al*.[9] developed a correlation for the mixing index for a size-variant and equal-density system of particles as:

$$I_M = K \times \left(\frac{d\overline{\mathrm{p}}}{d_{\mathrm{F}}}\right)^k \times \left(\frac{U}{U - U_{\mathrm{F}}}\right)^n \quad (1)$$

Cai *et al*.[10,11] developed a few correlations for prediction of 'U_c' for binary solids systems in fluidized

**Correspondence to*: Y. K. Mohanty, Department of Chemical Engineering, G.I.E.T., Gunupur, Rayagada, Orissa-765022, India.
E-mail: yashobantkumar@yahoo.com

beds with mono-density particles with relatively narrow size distribution. Buyevich and Kapbasov[12] studied the momentum equations governing vertical distribution of particles of different sizes and densities in a homogeneous fluidized bed and concluded that the conventional kinetic theory of gaseous mixtures, in which such force differences are usually not taken into account and the relative motion is conceived as a phenomenon of purely diffusional origin, is sufficient for expressing mean forces of interaction between the particulate components in terms of observable variables.

Qian *et al*.[13] studied particle mixing in rotating fluidized beds and concluded that for particles of the same material, two layers of particles do not mix until bubbles appear. Mixing occurs because of the difference in densities and fluidization properties of the two layers. This result was similar to that of Menon and Durian,[14] who concluded that bubbles are responsible for bulk motion of particles in a conventional fluidized bed. After the critical minimum fluidization velocity, particles inside the bed start to move radially and mixing occurs rapidly.

Sahoo and Roy[15] studied the mixing characteristics of linear homogeneous binary mixtures of regular particles (Geldart BD type) in a cylindrical gas–solid fluidized bed and developed a mathematical model for calculation of the mixing index:

$$I_M = 0.3725 \times \left(\frac{\overline{d_p}}{d_F}\right)^{0.3679} \times \left(\frac{h_B}{D_c}\right)^{-0.4864} \times \left(\frac{H_s}{D_c}\right)^{0.8258} \times \left(\frac{U}{U - U_F}\right)^{0.3084} \qquad (2)$$

Patil *et al*.[16] studied the influence of internal baffles on mixing characteristics and found that the bed without baffles showed a distinctive segregation nature. Internal baffles were effective in altering fluidization of biomass–sand mixtures.

Mohanty *et al*.[17] found that a distributor plate with a 10% open area of the column cross-section gives a better result (lower fluctuation and higher expansion) as compared to 6, 8 and 12% open areas of cross-section. Mohanty *et al*.[18] also found that at velocities more than twice the minimum fluidization velocity, better fluidization is achieved with secondary air supply.

Kumar and Roy[19] found that correlations using the dimensional analysis approach and artificial neural network (ANN) models can satisfactorily be used for the prediction of the bed expansion ratio, and that the ANN method represents the system behavior more accurately than the dimensional analysis approach. Wassermann[20] defined the ANN model as a computing system made up of a number of simple, highly interconnected nodes or processing elements that process information by its dynamic system response to external inputs. Davis[21] explained the statistical approach as one of the important methods for processing of experimental data due to its interaction effects among the variables and that fewer data are required for the development of the model equations. Naimer *et al*.[22] proposed a relationship for the calculation of the mixing index at different heights of a fluidized bed column.

Puyvelde[23] applied discrete elemental modeling to experimental data regarding mixing of solids in the transverse direction of a rotating kiln and found that the Froude numbers used in the model are not representative of those observed in the experimental work.

Gunaratnam *et al*.[24] presented a technique for generating concise neural network models of physical systems. Dimensional analysis techniques are used to make the information explicit, and a limited search in the neural network architecture space is then conducted to determine dimensionless representations of variables.

Delaplace *et al*.[25] studied the dimensional analysis of mixing time and reliability of modified Reynolds and mixing time numbers and proposed a planetary mixer particularly named as the TRIAXE system.

Baffi *et al*.[26] proposed a new methodology that is mathematically a more precise approach to evaluate the prediction intervals of the data generated from a nonlinear PH neutralization system for neural network models.

Chryssolouris[27] explained the importance of confidence interval prediction for neural network models. To estimate the error in predicting the true output, a first-order approximation of the error of the neural network model is estimated, which involves computing the Jacobian of the neural network outputs with respect to the weights.

Sahoo and Roy[28] studied the ANN approach to segregation characteristic of binary homogeneous mixtures in promoted gas–solid fluidized beds. The segregation characteristic of jetsam particles has been determined for different mixtures in terms of the segregation distance by empirically co-relating the result with the various system parameters through dimensional analysis and ANN approaches for both promoted and unpromoted beds.

Chen *et al*.[29] studied the effect of solid concentration on the secondary air-jetting penetration and found that the floater is more suitable to be operated in a spouted or a bubbling bed.

A survey of the literature reveals that attempts have been made to improve mixing of different particles of varying sizes and densities under different experimental conditions such as various types of promoters, distributor plates, etc. But the concept of using secondary air to enhance mixing has not yet been reported. Many thermal power-generating units are, of late, increasingly following the concept of circulating fluidized bed and are using secondary air in the fluidizer for improvement of the quality of fluidization and combustion. Owing to

DOI: 10.1002/apj

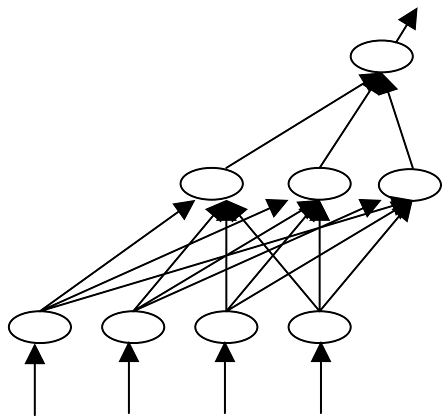

Figure 1. A typical three-layer neural network.

the scarcity of good-quality coal and an ever-increasing demand for electricity, the complete combustion of low-grade coal through introduction of secondary air is one of the best solutions.

The objective of the present work is to find a new technique for augmenting mixing expressed through a mixing index, and develop mathematical correlations for it (I_M) through four system parameters under different experimental conditions: only primary air, simultaneous primary and secondary air, disc promoter and rod promoter, using the factorial design approach. Computing through neural networks is one of the growing areas of artificial intelligence. It is also evident from the literature that the ANN approach can be suitably applied for the calculation of the same. In the present case, a software package for ANN in MAT LAB[30] has been used for the ANN simulation. Three typical layers, *viz.*,[1] input,[2] hidden and[3] output, have been chosen. Four nodes in the input layer, three neurons in the hidden layer and one node in the output layer have been taken as shown in Fig. 1.

EXPERIMENTAL

The experimental setup consists of an air compressor of adequate capacity, an air accumulator for storage of air at constant pressure and a silica gel column placed after the accumulator to arrest moisture. The schematic representation of the experimental setup is shown in Fig. 2. Rotameters have been used to measure the airflow rates. The calming section consisting of a cylindrical portion followed by a truncated conical bottom, and a distributor plate having a free area of 10% of the column cross-section is fixed at its top. The fluidizer is a transparent Perspex column 99 mm in internal diameter and 960 mm in height, with one of its ends fixed to the Perspex flange. Two pressure tappings have also been provided to measure the bed pressure drop through a differential manometer, in which carbon tetrachloride is used as the manometric fluid.

Five rods each of 4 mm diameter and 600 mm height have been taken in the case of the rod-type promoter and 10 circular discs each of 2 mm thickness and 60 mm diameter with a spacing of 50 mm have been taken in the case of the disc promoter. The supply of secondary air is made through a sparger pipe of 1 mm orifice diameter and 2 mm pitch.

Experiments were carried out by supplying primary air from below and secondary air (which is only a fraction (a maximum of 0.2) of the primary air supplied through the side ports of column in the middle of each static bed) through a pipe having fine holes directed only towards the top of the column like a sparger pipe as shown in Fig. 3. Two promoters, one rod type and one disc type (as shown in Fig. 4), were also used for the experimentation.

Experiments were carried out at four different conditions:

1. Primary air supply (unpromoted)
2. Using the rod promoter

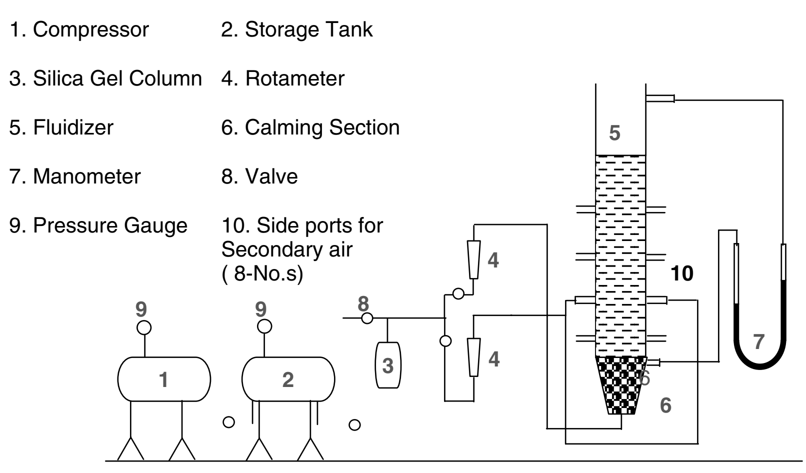

Figure 2. Schematic representation of the experimental setup.

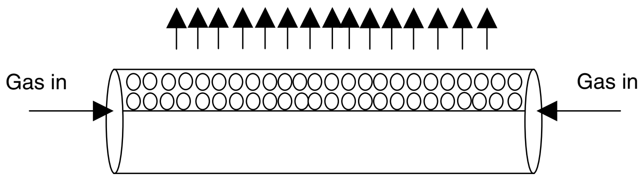

Figure 3. Schematic representation of air distributor for secondary air, 1 mm orifice diameter and 2.0 mm pitch.

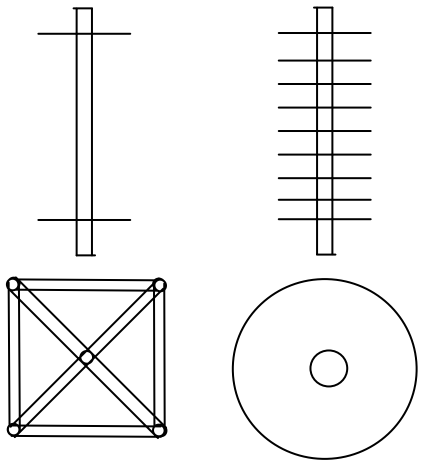

Figure 4. Schematic representation of rod- and disc-type promoters.

3. Using the disc promoter and
4. Simultaneous primary and secondary air supply (unpromoted).

In order to fluidize the entire bed material, the secondary airflow begins some time after the minimum fluidization condition is reached with the primary air. The variables affecting the mixing index are static bed height, particle density, particle size and velocity of air. The scope of the experiment is presented in Table 1. The total number of experiments required at two levels (minimum and maximum) for four variables is 16 for responses in the case of factorial design method[21]. Each experiment is repeated three times and the average of three values is reported as the response value. The various values of a factor examined in an experiment are known as levels. The set of levels of all factors employed in a given trial is called the treatment or treatment combination. The treatment combination gives a full description of the conditions under which the trial is carried out, insofar as these are affected by the various factors being studied. The numerical result of a trial based on a given treatment is called the response corresponding to that treatment.

Experiments were carried out by taking four different bed materials: iron, coal, dolomite and laterite. A 50 : 50 mixture (by weight) was taken for experimentation. The mixture was initially well mixed and then charged into the column, and then fluidized at varying airflow rates. Experiments were also carried out with primary and simultaneous primary and secondary air supplies.

During fluidization, samples were collected through the side ports on diametrically opposite sides at different heights of the fluidizer (intervals of 4 cm from the distributor plate, which is diametrically opposite to the secondary air inlet) for promoted, primary,

Table 1. Scope of the experiment.

Properties of the bed materials				
Materials	$d_p \times 10^3$, m			$\rho_s \times 10^{-3}$, kg/m^3
Dolomite	0.55, 0.725, 1.3			2.817
Laterite	0.55, 0.725, 1.3			3.47
Iron	0.55, 0.725, 1.3			4.4
Coal	0.55, 0.725, 1.3			1.6
Density of fluid, ρ_f	1.18 kg/m^3 at 25 °C			
Diameter of column, D_c	0.099 m			
Bed parameter				
Initial static bed height, $h_s \times 10^2$, m 8, 10, 12, 14				
Heights at which samples collected, $h_B \times 10^2$, m 4, 8, 12, 16, 20				
Flow property				
Materials	$h_S \times 10^2$	Average particle size, m	u_{mf}, m/s	u_f, m/s
Coal + iron	8	0.00055	0.504	1.08–2.16
Coal + iron	14	0.00055	0.648	1.08–2.16
Coal + iron	8	0.000725	0.576	1.08–2.16
Coal + iron	14	0.000725	0.72	1.08–2.16
Laterite + iron	8	0.00055	0.72	1.08–2.16
Laterite + iron	14	0.00055	0.864	1.08–2.16
Laterite + iron	8	0.000725	0.792	1.08–2.16
Laterite + iron	14	0.000725	0.936	1.08 to 2.16
Dolomite + iron	8	0.00055	0.648	1.08 to 2.16
Dolomite + iron	14	0.00055	0.792	1.08 to 2.16

DOI: 10.1002/apj

and simultaneous primary and secondary air supplies. Homogeneous mixtures with respect to their particle sizes and densities were considered for experimentation. Particles of different densities were separated through a magnetic separator, while those of different sizes through different sieves. The weights were taken in an electronic balance for the calculation of jetsam (for particles having higher densities and larger seizes) and flotsam (for particles having lower densities and smaller seizes) percentages, and then the mixing index values calculated.

DEVELOPMENT OF MODELS

Many experimental situations require the examination of the effects of varying two or more factors. In many cases it is not possible to vary more than one factor at a time, but all combinations of the different factor levels (Table 2) must be examined in order to elucidate the effect of each factor and the possible ways in which each factor may be modified by the variation of the factors. In the analysis of the experimental results, the effect of each factor can be determined with the same accuracy and the interaction effects between the factors can also be evaluated.

In the present work, the mixing index (I_M) at different heights has been calculated by using the following expression (Naimer *et al.*,[22]):

$$I_M = \frac{X^*}{\overline{X}_{bed}} \tag{3}$$

The mixing index (I_M) varies with the static bed height, particle size, density and gas mass velocity (Sahoo and Roy,[15]). The effect of all these four variables was studied with primary air supply, rod-promoted bed, disc-promoted bed and simultaneous primary and secondary air supply.

A mathematical model was also developed for prediction of the mixing index. The model equations are assumed to be linear and take the general form:

$$I = a_0 + \sum_i a_i A_i + \sum_i \sum_j a_{ij} A_i A_j + \sum_i \sum_j \sum_k a_{ijk} A_i A_j A_k + \sum_i \sum_j \sum_k \sum_l a_{ijkl} A_i A_j A_k A_l \tag{4}$$

where 'I' stands for the mixing index; A_i, A_j, A_k and A_l are factorial design symbols; i, j, k and l vary from 1 to 4 such that $i < j < k < l$.

The coefficients are calculated by Yate's technique,

$$a_i = \sum \alpha_i y_i / N \quad \ldots. \tag{5}$$

where a_i is the coefficient, y_i is the response, α_i is the level of variables and N is the total number of treatments (Davis[21]). The experimental data based on factorial design, nature of the effects and its analysis are presented for the mixing index in Tables 2 and 3 for primary air, disc promoter, rod promoter and simultaneous primary and secondary air supplies, respectively.

The levels of variables are calculated as:

$$\left.\begin{array}{l} A_1 : \text{Level of static bed height} = (A_1 - 1.95)/1.55 \\ A_2 : \text{Level of density} = (A_2 - 2.938)/0.396 \\ A_3 : \text{Level of particle size} = (A_3 - 0.0064)/0.0009 \\ A_4 : \text{Level of velocity} = (A_4 - 2.7)/0.6 \end{array}\right\} \tag{6}$$

The effect of a factor is the change in response produced by a change in the level of that factor. When a factor is examined at two levels only, the effect is simply the difference between the average response of all trials carried out at the first level of the factor and that of all trials at the second level.

Equations (7),(8),(9) and (10) have been developed for the mixing index under four different experimental conditions (neglecting smaller coefficients):

Table 2. Factorial design analysis.

Sl. no.	Name of the variable	Variable general symbol	Factorial design symbol	Minimum level (−1)	Maximum level (+1)	Magnitude of variables
1	Static bed height	h_s/h_B	A_1	0.4	3.5	2.0, 1.0, 0.67, 0.5, 0.4, 2.5, 1.25, 0.83, 0.625, 3.0, 1.5, 0.75, 0.6, 3.5, 1.75, 1.16, 0.875, 0.7
2	Density	ρ_{Mavg}/ρ_f	$A_2 \times 10^{-3}$	2.542	3.334	2.542, 2.923, 3.334
3	Particle size	d_{Pavg}/D_c	A_3	0.0055	0.0073	0.0055, 0.0073, 0.013
4	Velocity	u_f/u_{mf}	A_4	2.1	3.3	2.1–4.28

DOI: 10.1002/apj

Table 3. Analysis of mixing index data.

Sl. No.	A_1	$A_2 \times 10^{-3}$	A_3	$A_4(u_f/u_{mf})$	I_{MP}	I_{MR}	I_{MD}	$A_4\ (u_p/u_s)$	I_{MS}
				Experimental				Experimental	
1	0.4	2.542	0.0055	2.1	0.7404	0.764	0.802	2.1	0.9042
2	3.5	2.542	0.0055	2.1	1.1722	1.1032	1.083	2.1	1.0054
3	0.4	3.334	0.0055	2.1	0.7934	0.803	0.8426	2.1	0.9334
4	3.5	3.334	0.0055	2.1	1.042	1.0062	1.0226	2.1	1.0004
5	0.4	2.542	0.0073	2.1	0.705	0.735	0.7602	2.1	0.801
6	3.5	2.542	0.0073	2.1	1.1942	1.1522	1.1156	2.1	1.063
7	0.4	3.334	0.0073	2.1	0.763	0.7958	0.8032	2.1	0.821
8	3.5	3.334	0.0073	2.1	1.1134	1.0878	1.0456	2.1	1.021
9	0.4	2.542	0.0055	3.3	0.7402	0.7812	0.8402	3.3	0.8926
10	3.5	2.542	0.0055	3.3	1.0604	1.053	1.0492	3.3	1.02
11	0.4	3.334	0.0055	3.3	0.8002	0.8214	0.852	3.3	0.9034
12	3.5	3.334	0.0055	3.3	1.0602	1.0218	1.0326	3.3	1.006
13	0.4	2.542	0.0073	3.3	0.713	0.743	0.775	3.3	0.8624
14	3.5	2.542	0.0073	3.3	1.1346	1.1028	1.075	3.3	1.053
15	0.4	3.334	0.0073	3.3	0.7804	0.8038	0.8356	3.3	0.863
16	3.5	3.334	0.0073	3.3	1.042	1.061	1.0396	3.3	1.0112

Columns indicating A_1, A_2 and A_3 are common.

For disc-promoted bed:

$$I_{MD} = 0.9358 + 0.1222\ A_1 - 0.00165\ A_2 - 0.00465\ A_3 + 0.00152\ A_4 - 0.0211\ A_1A_2 + 0.0157\ A_1A_3 - 0.01\ A_1A_4 \quad (7)$$

For rod-promoted bed:

$$I_{MR} = 0.9272 + 0.1462\ A_1 - 0.0021\ A_2 + 0.0079\ A_3 - 0.0037\ A_4 - 0.027\ A_1A_2 + 0.019\ A_1A_3 - 0.01\ A_1A_4 \quad (8)$$

For primary air (unpromoted):

$$I_{MP} = 0.9284 + 0.1739\ A_1 - 0.004\ A_2 + 0.0022\ A_3 - 0.012\ A_4 - 0.0338\ A_1A_2 + 0.0163\ A_1A_3 - 0.016\ A_1A_4 + 0.008\ A_2A_4 \quad (9)$$

For simultaneous primary and secondary air (unpromoted):

$$I_{MS} = 0.9477 + 0.0751\ A_1 - 0.00241\ A_2 - 0.0108\ A_3 + 0.0036\ A_4 - 0.0099\ A_1A_2 + 0.0249\ A_1A_3 \quad (10)$$

In the present work, the ANN model based on supervised feed-forward neural network with back propagation algorithm for the calculation of mixing index in the case of primary air, simultaneous primary and secondary air, rod promoter and disc promoter has been developed. Factorial design techniques are used initially to represent the dependent and independent variables/parameters through model equations. Later on, an ANN model is developed to test these data for its authentication. In all the cases, three-layer feed-forward ANN structures (input layer × hidden layer × output layer) have been tested at constant epochs (cycles), learning rate, error goal and net trained parameter. The

Table 4. Selected structures of neural network models.

Net train parameter: 100
Percentage set learning rate: 1.0
Net train parameter learning: 1.0
Percentage set error goal: 0.001
Net train parameter epochs: 20 000
Performance: 0.00141672

Bed particulars	Input nodes	Hidden nodes	Output nodes	No. of cycles
Primary air	4	3	1	20 000
Secondary air	4	3	1	20 000
Rod promoter	4	3	1	20 000
Disc promoter	4	3	1	20 000

DOI: 10.1002/apj

selected structures of the ANN model is considered for training of the input and output (after normalizing the data, i.e. values in the range of 0.1–0.999) data in each case as shown in Table 4. The network is trained for a given set of input and target data sets. These data were obtained from the experimental observations. The network is trained with 100 data sets in each case, where each set consists of four system parameters and the corresponding experimental value of the mixing index.

For a desired degree of confidence (namely, for a given probability), a confidence interval is a prediction of the range of the output of a model where the actual value exist. Discrepancy between the true output and the observed output of the system may exist, due to inaccuracies in measurement of the output. Such an estimate may be used to predict the domain of the input over which a neural network model will adequately model the output of the system. The representation of the system is given by Eqn (4). The error value is the difference between the true output value and the neural network output, arising from the limitations of the model to capture the unobservable and uncontrollable error.

The data were scaled down and then the network was exposed to those scaled data sets. The network weights were updated using the back propagation algorithm. The algorithm is implemented using the MAT LAB[30] programming language. In this back propagation, the network corrects its weights to decrease the observed error as described by Kumar and Roy[19] and Wassermann.[20] The network structure together with the learning rate was varied to obtain an optimum structure with a view to minimize the mean percentage set error goal to 0.001. The training data sets were impressed repeatedly for a maximum of 20 000 epochs till the percentage set error goal is achieved. The network with the weights obtained from the training is now exposed to the prediction data set and thereby 100 sets of output data were computed. Then the output data were multiplied with the normalized data to get the final output.

RESULTS AND DISCUSSION

The flow of secondary air begins after the bed starts to fluidize because of primary air supply through the bottom of the fluidizer. It has been observed that the secondary air exerts an axial thrust on the bottom of the bed, and owing to this effect the primary air supply is maintained at more than the minimum fluidization velocity, i.e. $u_{mf} + 0.144$ for all the experiments. If this extra amount of primary air (0.144 m/s, experimentally found) is not supplied, then the lower half of the bed will not fluidize properly, i.e. the bed will behave like a fixed bed. For any bed material this is the minimum required extra amount of air that has to be supplied in addition to the amount of minimum fluidization velocity, i.e. u_{mf}. It has been observed that the introduction of secondary air enhances mixing among the particles of a wide range of sizes and densities due to greater turbulence in the bed.

For fluidized bed conditions, the samples have been drawn from the side ports made on either side (diametrically opposite) of the column (maintaining same velocity ratios, i.e. u_f/u_{mf} and u_p/u_s as indicated in Table 3) and analyzed on the basis of the assumption of uniform concentration for a particular layer of particles across the cross-section of the column at any height. Apart from this, the diameter of the column, i.e. 9.9 cm, also supports the assumption. Then the samples have been separated through a magnetic separator and then the weights of the flotsam and jetsam particles taken in an electronic digital balance.

It is clearly evident from Eqns (7),(8),(9) and (10) that the effect of the variable 'static bed height to the height at which samples are drawn' ($h_s/h_B = A_1$) is prominent as compared to the densities, particle sizes and gas velocities. In case of combined effects of variables, A_1 predominates over the other variables. During experimentation, the segregation tendency is clearly observed in the lower velocity ranges ($u_f < 2u_{mf}$) and the jetsam concentration decreases with an increase in the height of the column. It is also evident from Table 5 that the developed model gives approximately the same values as experimental values as compared to the model of Sahoo and Roy[15] for the same input data. The values of the mixing index in a few cases are more than 1 only when the jetsam concentration is less than 50%, which indicate segregation tendency.

It has been found form Eqns (7),(8),(9) and (10) that the mixing index is a direct function of bed heights and

Table 5. Comparison of mixing index for the same input data.

$d_p \times 10^3$	d_F	D_c	h_B	h_S	$U/(U - u_{mf})$	u_f/u_{mf}	I_{Mexp}	I_{Mcal} (Eqn (2))	I_{Mcal} (Eqn (9))
0.55	0.55	0.099	0.04	0.08	1.875	2.142	1.143	0.587	1.064
0.55	0.55	0.099	0.08	0.08	1.875	2.142	0.892	0.419	0.997
0.55	0.55	0.099	0.04	0.14	1.9	2.11	1.172	0.943	1.166
0.55	0.55	0.099	0.08	0.14	1.9	2.11	0.973	0.673	1.048
0.725	0.725	0.099	0.04	0.14	1.86	2.15	1.113	0.937	1.040
0.725	0.725	0.099	0.08	0.14	1.86	2.15	1.087	0.669	0.993
0.725	0.725	0.099	0.20	0.14	1.9	2.1	0.722	0.429	0.978

DOI: 10.1002/apj

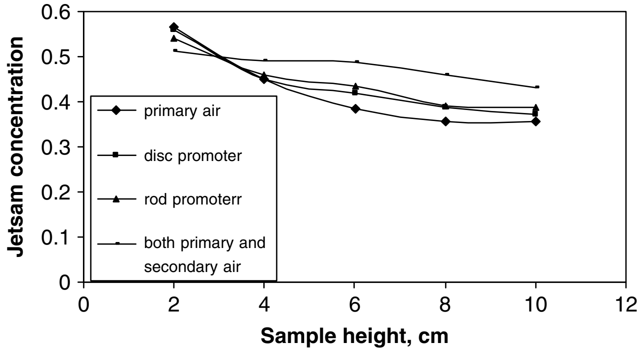

Figure 5. Effect of primary air, disc promoter, rod promoter and simultaneous primary and secondary air on mixing coal and iron: static bed height 0.14 m, $G_f = 2.55$ kg/m^2 s.

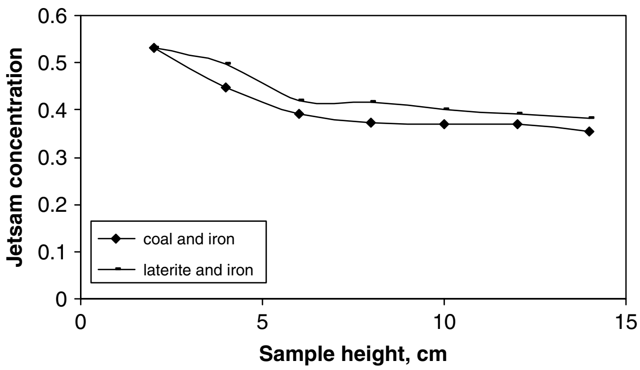

Figure 6. Effect of density on mixing: primary air, coal and iron, static bed height 0.14 m, $G_f = 2.55$ kg/m^{2}s.

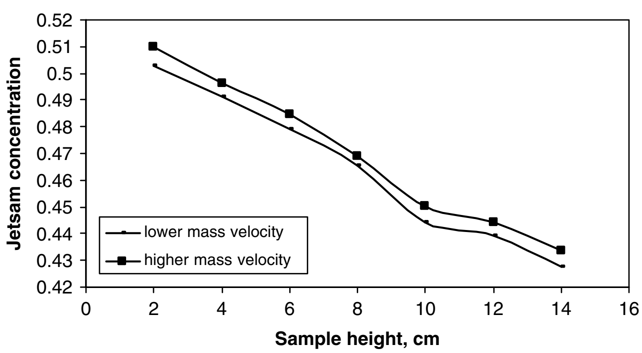

Figure 7. Effect of mass velocity on mixing: simultaneous primary and secondary air, coal and iron, static bed height 0.08 m, particle size 0.00055 m.

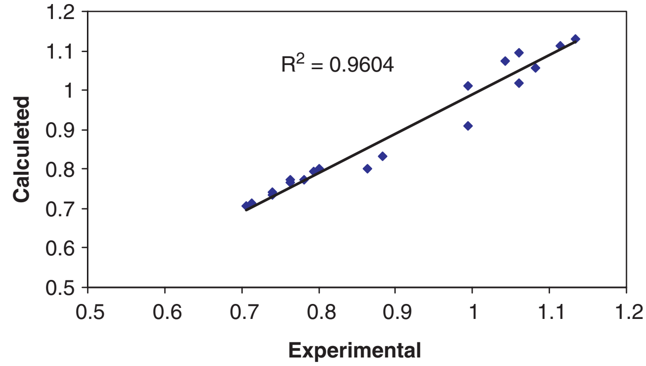

Figure 8. Comparison of mixing index values in the case of primary air supply. This figure is available in colour online at www.apjChemEng.com.

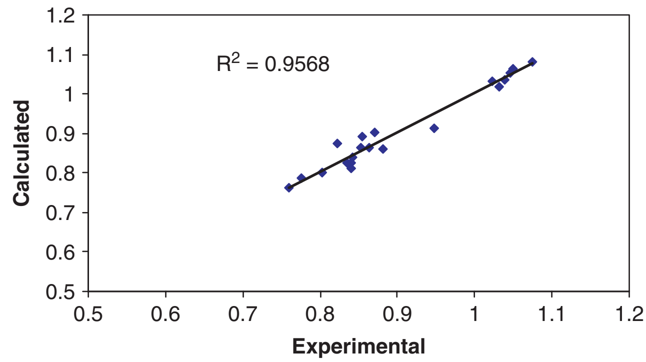

Figure 9. Comparison of mixing index values in the case of disc-promoted bed. This figure is available in colour online at www.apjChemEng.com.

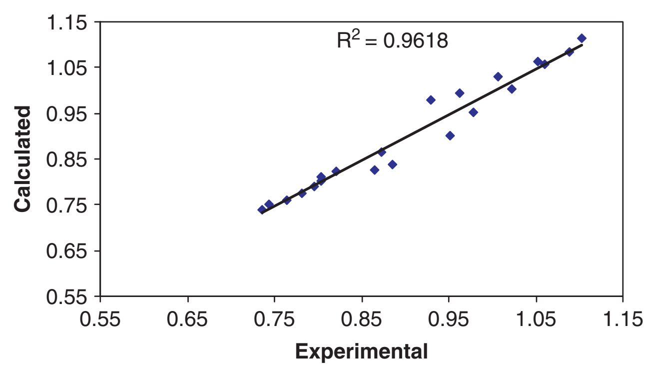

Figure 10. Comparison of mixing index values in the case of rod-promoted bed. This figure is available in colour online at www.apjChemEng.com.

an inverse function of densities in all the four cases. But the mixing index is an inverse function of particle sizes and a direct function of gas velocities for the disc-promoted bed and simultaneous primary and secondary air supply, whereas it is evident that in the case of only primary air supply and rod promoter, it is a direct function of particle sizes and an inverse function of gas velocities.

It has been observed that simultaneous primary and secondary air supply gives good mixing index values (jetsam and flotsam concentration of 0.5, i.e. $I_M = 1.0$ represents perfect mixing) owing to greater turbulence in the bed as compared to the other three conditions as evident form Fig. 5. It has also been found that the rod

DOI: 10.1002/apj

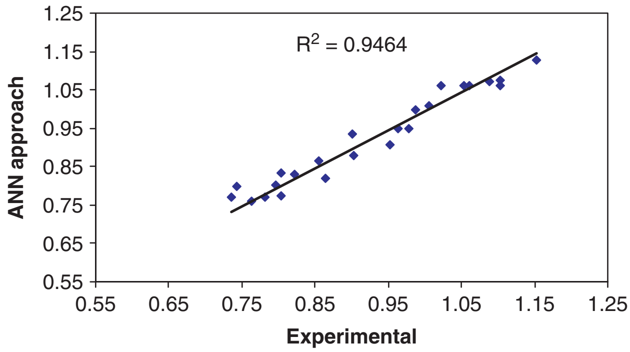

Figure 11. Comparison of mixing index values in the case of simultaneous primary and secondary air supplies. This figure is available in colour online at www.apjChemEng.com.

promoter is superior to disc promoter, as the latter provides intermittent resistance (provided with the disc) for which bubbles are not able to carry the jetsam particles to greater heights, and hence more segregation tendency develops. In the case of rod promoter, the resistance is offered both radially and axially but transport of some wake particles might occur through the gap between the column and rods, thereby causing better mixing of particles. The resistance offered by disc promoter dominates over that by the rod promoter. It is also evident from Fig. 6 that the particles with more homogeneity (laterite and iron) with respect to density gives better mixing as compared to less homogenous particles, i.e. coal and iron. The value of mixing index 1.0 indicates perfect mixing; deviation on either side represents the development of segregation tendencies. It is evident from Fig. 7 that with an increase in velocity better mixing is obtained. Comparisons of mixing index values obtained from the developed factorial design model with the experimental values are presented in Figs 8, 9 and 10. The R^2 values shown on the graph indicate that it is well within the accepted region of the engineering limit. The present experimentation considered particles with a wide range of sizes and densities. Hence, the developed equations can be successfully utilized for future work.

Neural network models have been used as a predictor for different physical systems. The predicted values of mixing index using ANN and factorial design approaches have been compared with the experimental values for simultaneous primary and secondary air supplies as shown in Fig. 11. The R^2 value obtained in this case is also well within the acceptable region. It has also been observed that the ANN approach holds good for all the velocity ranges, which is an authentication to the present model and experimentation.

The standard deviations for mixing index (in percentage) have been found to be ± 3.47, ± 5.64, ± 6.6 and ± 4.8 for disc-type promoter, rod-type promoter, primary air, and simultaneous primary and secondary air supplies, respectively, in the case of factorial design approach.

CONCLUSIONS

The developed correlations by the factorial design approach have been completely authenticated by the ANN models. The developed models can be used widely for analyzing the mixing and segregation characteristics of the homogenous/heterogeneous binary mixtures of particles over a good range of operating parameters. Mixing index decreases with increase in the height of the column measured from the distributor plate, which is in good agreement with the experimental data. Of the two types of promoters, disc and rod, the latter type has been found to be superior. However, during simultaneous primary and secondary air supplies, the best mixing is obtained. Furthermore, it has been observed that the mixing performance under four different conditions is in the following order: primary air supply (unpromoted), disc type, rod type and simultaneous primary and secondary air supply. In the higher velocity range of air, better mixing is obtained, whereas better segregation is obtained in the lower velocity range ($u_f < 2u_{mf}$). Hence, simultaneous primary and secondary air supply may be considered as the best method (instead of using bed internals) to augment mixing among particles of varying densities. Factorial design and ANN approaches can be suitably used for prediction of mixing index.

NOMENCLATURE

C_j	Concentration of jetsam particles at any height in the bed (amount of jetsam particle in the sample drawn at a height in kg/amount of that in the original mixture in kg)
d_F	Diameter of flotsam particle, m
d_p	Particle size of the mixture, m
$\overline{d_p}$	Average particle size of the mixture, m
D_c	Diameter of column, m
u_f	Velocity corresponding to fluidization, m/s
u_{mf}	Velocity corresponding to minimum fluidization, m/s
u_p	Velocity of the medium due to primary air $= u_{mf} + 0.144$, m/s
u_s	Additional velocity of the fluidizing medium due to secondary air, m/s
h_B	Height of particles layer in the bed from the distributor, m
H_s	Initial static bed height, m

DOI: 10.1002/apj

h_s	Initial static bed height, m
I_M	Mixing index, dimensionless
I_{MD}	Mixing index in the case of disc promoter
I_{MR}	Mixing index in the case of rod promoter
I_{MP}	Mixing index in the case of primary air supply
I_{MS}	Mixing index in the case of simultaneous primary and secondary air supply
U	Superficial velocity of the fluidizing medium, m/s
U_c	Transition velocity from bubbling to turbulent fluidization, m/s
U_F	Minimum fluidization velocity of the flotsam particles, m/s
X^*	Percentage of jetsam particles in any layer
X_{bed}	Percentage of jetsam particles in the bed
A_1, A_2, A_3, A_4	Factorial design symbols

Greek letters

ρ_f	Density of fluid, kg/m^3
ρ_s	Density of solid particle, kg/m^3
ρ_{Mavg}	Average density of solid particle, kg/m^3

Subscripts

cal	Values calculated from the developed models
exp	Values obtained from the experiment

REFERENCES

[1] L.G. Gibilaro, P.N. Rowe. *Chem. Eng. Sci.,* **1974;** *29*, 1403–1412.

[2] J.R. Grace. In *Gas Fluidization Technology* (Ed.: D. Geldart), Wiley: New York, **1986;** pp.287–341.

[3] P.N. Rowe, A.W. Nienow. *Chem. Eng. Sci.,* **1975;** *30*, 1365–1369.

[4] M.P. Aznar, F.A. Gracia-Gorria, J. Corella. *Int. Chem. Eng.,* **1992;** *32*, 95–102.

[5] H.T. Bi, P.J. Jiang, R.H. Jean, L.S. Fan. *Chem. Eng. Sci.,* **1992;** *47*, 3113–3124.

[6] A.W. Nienow, N.S. Naimer, T. Chiba. *Chem. Eng. Commun.,* **1987;** *62*, 53–66.

[7] A.C. Hoffmann, L.P.B. Fanssen, J. Pris. *Chem. Eng. Sci.,* **1993;** *48*, 1583–1592.

[8] K. Noda, S. Uchida, T. Makino, H. Kamo. *Powder Technol.,* **1986;** *46*, 149–154.

[9] L.T. Fan, Y. Chen, F.S. Lai. *Powder Technol.,* **1990;** *61*, 255–287.

[10] P. Cai, Y. Jin, Z.Q. Yu, Z.W. Wang. *AIChE J.,* **1990;** *36*, 955–956.

[11] P. Cai, Y. Jin, Z.Q. Yu, L.S. Fan. *Ind. Eng. Chem. Res.,* **1992;** *31*, 632–635.

[12] Y.A. Buyevich, S.K. Kapbasov. *Chem. Eng. Sci.,* **1994;** *49*, 1245–1257.

[13] G. Qian, I. Bagyi, R. Pfeffer, H. Shaw. *Part. Technol. Fluidization,* **1999;** *45*, 1401–1410.

[14] N. Menon, D.J. Durian. *Phys. Rev. Lett.,* **1997;** *79*, 3407–3413.

[15] A. Sahoo, G.K. Roy. *Powder Technol.,* **2005;** *159*, 150–154.

[16] K.N. Patil, R.L. Huhnke, D.D. Bellmer. Agricultural Engineering International: the CIGR Ejournal, Manuscript EE 06 016, April **2007;** Vol.IX.

[17] Y.K. Mohanty, K.C. Biswal, G.K. Roy. *Indian Chem. Eng.,* **2007;** *49*(1), 1–10.

[18] Y.K. Mohanty, K.C. Biswal, G.K. Roy. *Indian Chem. Eng.,* **2007;** *49*(2), 134–142.

[19] A. Kumar, G.K. Roy. *J. Inst. Eng. (India),* **2004;** *85*, 12–16.

[20] P.D. Wassermann. *Neural Computing Theory and Practice*, Van Nastrank Reinhold: New York, **1989**.

[21] O.L. Davis. *Design and Analysis of Industrial Experiments*, 2nd edn, Longman Publishers: London, **1978**.

[22] N. Naimer, T. Chiba, A.W. Nienow. *Chem. Eng. Sci.,* **1982;** *37*, 1047–1057.

[23] D.R.V. Puyvelde. *Chem. Eng. Sci.,* **2006;** *61*, 4462–4465.

[24] D.J. Gunaratnam, T. Degroff, J.S. Gero. *Appl. Soft Comput.,* **2003;** *2*, 283–296.

[25] G. Delaplace, R.K. Thakur, L. Bouvier, C. Andre, C. Torrez. *Chem. Eng. Sci.,* **2007;** *62*, 1442–1447.

[26] G. Baffi, E. Martin, J. Morris. *Chemom. Intell. Lab. Syst.,* **2002;** *61*, 151–165.

[27] G. Chryssolouris, M. Lee, A. Ramsey. *IEEE Trans. Neural Netw.,* **1996;** *7*, 229–232.

[28] A. Sahoo, G.K. Roy. *Powder Technol.,* **2007;** *171*, 54–62.

[29] J. Chen, X. Lu, H. Liu, J. Liu. *Powder Technol.,* **2008;** *185*(2), 164–169.

[30] MAT LAB Version, 6.5.0.18093a Release 13.

DOI: 10.1002/apj